Journal of Porphyrins and Phthalocyanines

Article Title: **Dipyrrolylnaphthyridine-based Schiff-base cryptands and their selective gas adsorption properties**

Author(s): **Fei Wang, Eric Sikma, Zhiming Duan, Chuanhu Lei, Zhan Zhang, Simon M. Humphrey, Jonathan L. Sessler**

DOI: **10.1142/S1088424619501396**

To be cited as:

Fei Wang, Eric Sikma, Zhiming Duan, Chuanhu Lei, Zhan Zhang, Simon M. Humphrey, Jonathan L. Sessler, Dipyrrolylnaphthyridine-based Schiff-base cryptands and their selective gas adsorption properties, *Journal of Porphyrins and Phthalocyanines*, doi: 10.1142/S1088424619501396

Received: *7 September, 2019*
Accepted: *20 September, 2019*

Dipyrrolylnaphthyridine-based Schiff-base cryptands and their selective gas adsorption properties

Fei Wang,[a,b] Eric Sikma,[d] Zhiming Duan,[b] Chuanhu Lei,[b] Zhan Zhang,[*b,c] Simon M. Humphrey,[*d] Jonathan L. Sessler,[*b,d]

[a] *School of Materials Science and Engineering, Shanghai University, Shanghai 200444, China.*
[b] *Center for Supramolecular Chemistry & Catalysis, Shanghai University, Shanghai 200444, China.*
[c] *College of Chemistry and Materials Science, South-Central University for Nationalities, Wuhan 430074, China*
[d] *Department of Chemistry, The University of Texas at Austin, Texas 78712-1224, United States.*

Dedicated to Professor Atsuhiro Osuka on the occasion of his 65th birthday.

Received date (to be automatically inserted after your manuscript is submitted)
Accepted date (to be automatically inserted after your manuscript is accepted)

ABSTRACT: Presented here is the synthesis of three new Schiff-base cryptands, **4**–**6**. Dynamic covalent imine bond formation via the condensation of a dialdehyde (**7** or **8**) with two different tris-amines allowed for the preparation of **4**–**6** in 84%, 80%, and 83% yield, respectively. These systems were characterized by NMR spectroscopy, mass spectra, and, in the case of **5**, single crystal X-ray diffraction analysis. These cages act as selective CO_2 gas adsorbing materials in the solid state.

KEYWORDS: synthesis, characterization, Schiff-base cryptand, gas adsorption.

*Correspondence to: Zhan Zhang, email: zhangzhan5@foxmail.com; Simon M. Humphrey, email: smh@cm.utexas.edu; Jonathan L. Sessler: sessler@cm.utexas.edu.

INTRODUCTION

Interest in three-dimensional structurally defined organic molecules has increased rapidly in recent years. This blossoming reflects in part the fact that such systems have become relatively accessible through dynamic covalent chemistry (DCC) approaches involving the formation of imines from amines and aldehydes [1], boronic esters from boronic acids and diols [2], disulfides from thiols [3], and several other reversible bond formation reactions [4]. Typically, spatially defined systems resulting from these approaches involve core constructive elements with bonds to at least one heteroatom [5]. Nevertheless, it has proved possible to create a variety of cryptand-like structures with internal voids, persistent shapes, and rigid, three-dimensional frameworks that are chemically and thermally robust [6]. However, extensions of this chemistry that allows functional groups to be accommodated within the internal pores remains a largely unmet challenge. This could reflect the difficulty associated with the design and synthesis of suitable precursors for constructing such cryptand-like systems. We and others have considered that the use of pyrrolic building blocks may provide a

means of overcoming these preparative limitations. Recently, Setsune and coworkers described a cryptand-like porphyrinoid **1** assembled from three dipyrrylpyridine chains. The result is a system characterized not only by an inner void but also three crevice-like substructures [7]. Our own group has recently prepared several related systems (e.g., **2** and **3**) which showed open cavities as inferred from solid state structural analyses and which act as selective CO_2 gas adsorbing materials in the solid state [8]. In this study, we report the result of efforts to extend the key linking chain from a dipyrrylpyridine derivative (**7**) to one incorporating a dipyrrylnaphthyridine (**8**) [9]. These two building blocks have allowed for the construction of three new cage systems **4**–**6** (Fig. 1). All three systems were characterized by NMR spectroscopy, mass spectra, and in the case of **5**, single crystal X-ray analysis. These cages were used for gas adsorption studies in the solid state and found to act as selective CO_2 gas adsorbing materials.

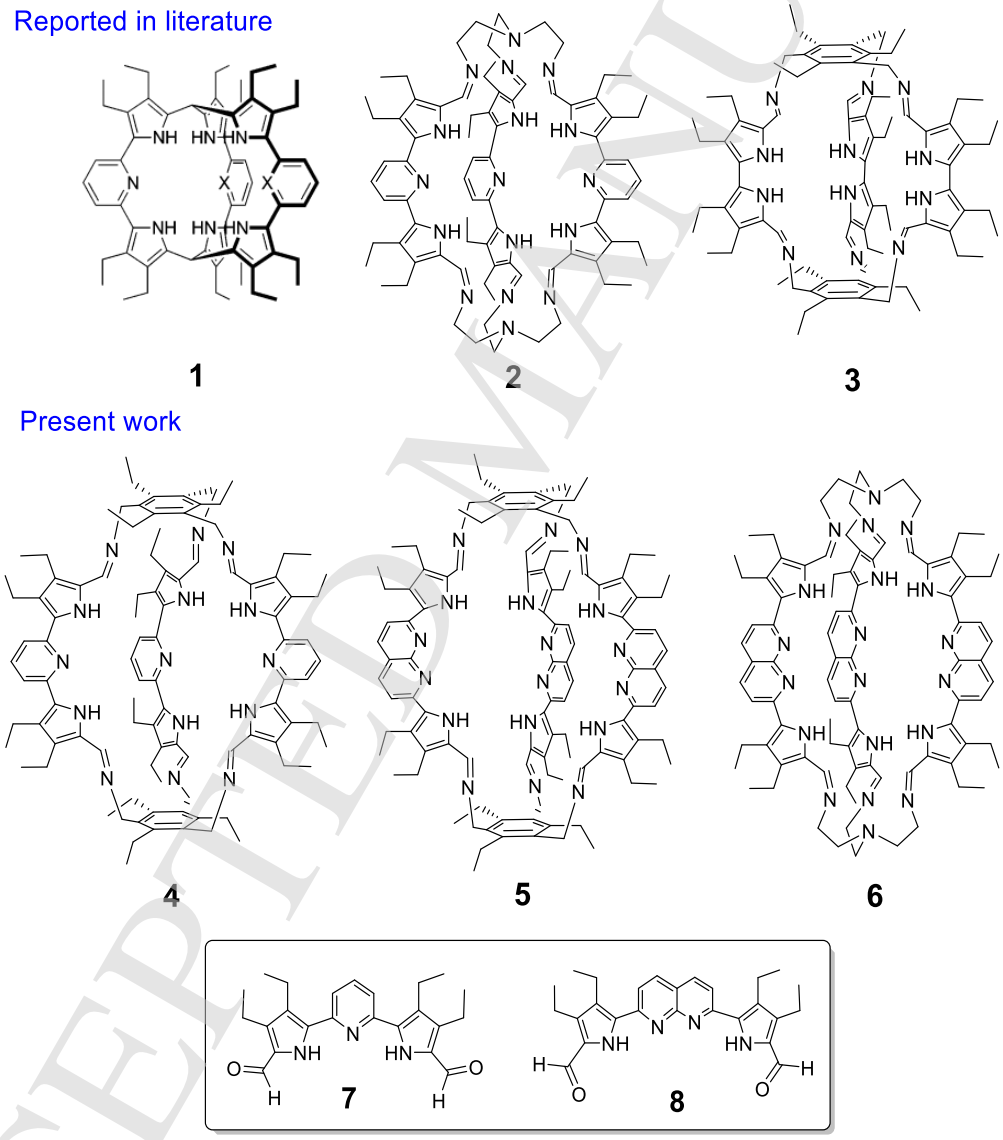

Fig. 1. Chemical structures of various cryptands (**1**-**6**). Inset: Chemical structures of aldehyde precursors **7** and **8** used to synthesize **4**, **5,** and **6** in the context of the present study.

RESULTS AND DISCUSSION

Considered from a synthetic point of view, the limitation to obtaining a new analogue of 3 (such as **5** and **6**) containing naphyridine motifs is the preparation of a suitable diformyl dipyrrolylnaphthyridine precursor. In the case of **2**, the diformyl dipyrrylpyridine **7** allowed access to the three-dimensional structure via condensation with an appropriately chosen trisamine. Precursor **7** was constructed through a procedure involving Suzuki coupling [10]. We thus considered it likely that the β-substituted naphthyridine-dipyrrole, **8**, could be obtained in a similar fashion. In fact, as detailed below, this expectation was realized.

The synthesis of **8** was achieved via a Pd-catalyzed Suzuki cross coupling after investigating a several possible strategies. As shown by Scheme 1, our starting material was the well-known porphyrin precursor, 3,4-diethyl pyrrole **9**. Routine formylation of **9** under Vilsmeier-Haack conditions produced **10** efficiently [11]. Subsequent halogenation with 1.2 equivalent of N-iodosuccinimide (NIS) [12] produced **11** in excellent yield. However, the next step, involving borylation under modified Miyaura's conditions only gave **12** in yields of 50−70%. Usually the pyrrolylboronic acid pinacol ester **12** was obtained in the form of reddish-brown oil. Storing at low temperature for an extended period then gave a reddish-brown solid. Suzuki cross-coupling of **12** with 2,7-dibromo-1,8-naphthyridine at 85 °C generated the key fluorescent precursor **8** in moderate yield (45%). Although the yield was not high, the coupling reaction leading to **8** could be carried out conveniently on 3 g scale, which provided sufficient material to allow the synthesis of the target cryptands **4**, **5** and **6** to be completed.

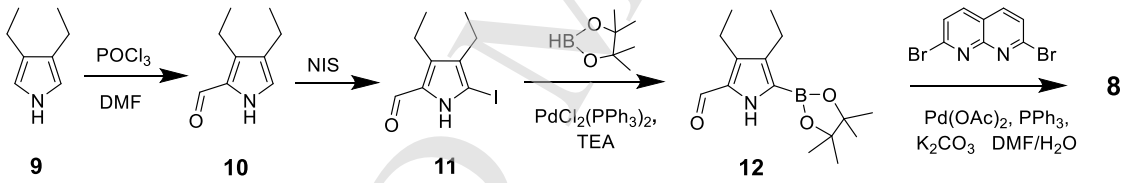

Scheme 1. Synthesis of dialdehyde precursor **8**.

With dialdehydes **7** and **8** in hand, we turned to the challenge of preparing the cryptands **4**–**6** (Scheme 2). We initially employed the so-called slow addition strategy that is commonly used to favor the formation of well-defined architectures. We examined the order of addition and found adding a capping triamine to a solution of dialdehyde in appropriately chosen dry solvents yielded cleaner product than when the addition was carried out in the opposite order. After the completion of addition, the reaction mixture was allowed to sit so as to favor so-called error correction in the framework architecture via dynamic bonding. In this way, and using methanol as the solvent, cryptand **4** was synthesized at room temperature from dialdehyde **7** and triamine **13** in excellent yield (84%). The product precipitated out of the methanol solution during the course of the reaction. This precipitation not only made purification simple, it also presumably served to drive the reaction towards completion. Using this same basic protocol, cryptands **5** and **6** were likewise synthesized in excellent yields (80% and 83%, respectively). The only difference was dry dichloromethane (DCM) was used to dissolve dialdehyde **8** because of its exceptionally poor solubility in methanol. It was subsequently found that simply

stirring a 2:3 mixture of a triamine (**13** or **14**) and a dialdehyde (**7** or **8**) in methanol at room temperature for two days also produced the desired product(s) in almost quantitative yield(s).

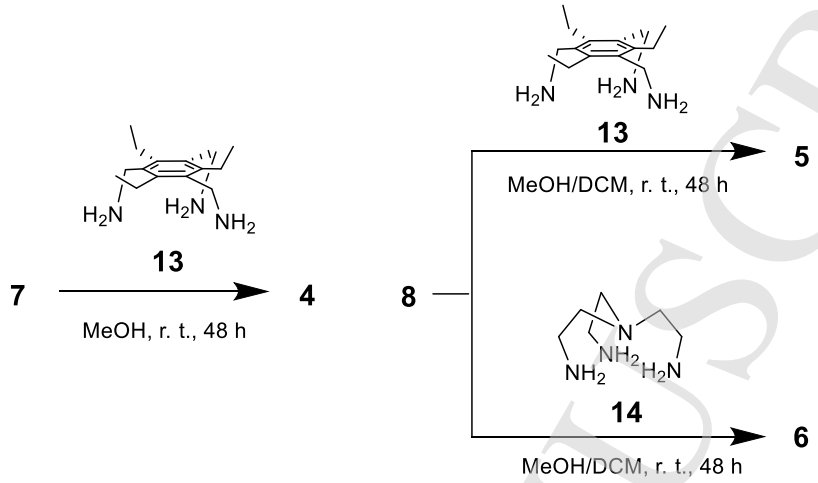

Scheme 2. Synthesis of cryptands **4**–**6**.

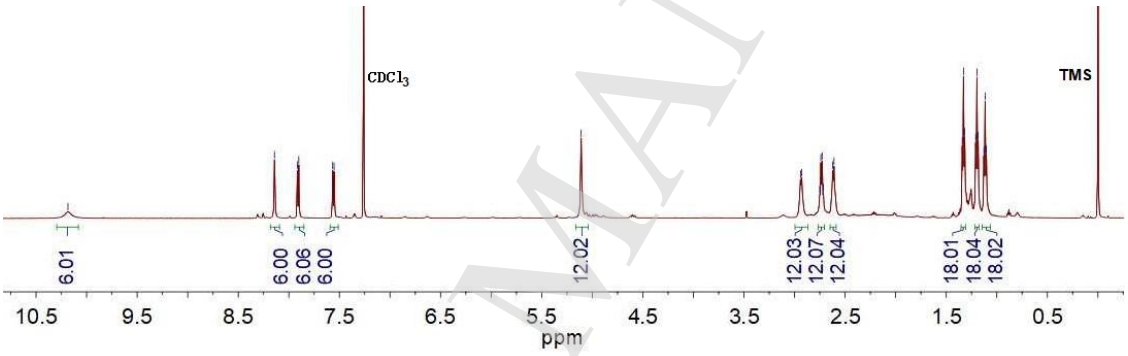

Fig. 2. ^{1}H NMR spectrum of cryptand **5** recorded in $CDCl_3$ at 298 K.

Products **4**–**6** were characterized initially on the basis of ^{1}H NMR spectroscopic and mass spectrometric (MS) analyses. The resulting data proved consistent with the proposed hexa-imine cryptand structures. In the case of the cryptand-like species **5**, for example, the ^{1}H NMR spectrum (Fig. 2) revealed a high degree of symmetry, at least in solution under the conditions of analysis. Moreover, in addition to signals ascribable to the pyrrole-naphthyridine-pyrrole subunits, a single peak in the aromatic region, a single peak at 4.7 ppm, and two coupled peaks (CH_2-CH_3) in the aliphatic region were observed. These latter sets of peaks are readily assigned to the fragment triamine **13**, whereas the signal in the aromatic area, combined with the disappearance of aldehyde CH proton signal, provides support for the conclusion that Schiff base formation took place. A signal corresponding to the expected formula ($C_{108}H_{126}N_{18}$) was also seen in the MS spectrum. We thus conclude that the cryptand-like product **5** was formed. Further support for this conclusion came from a single crystal X-ray diffraction analysis.

Yellowish rod-like single crystals of **5** were grown via slow diffusion of petroleum ether (PE) into a chloroform solution of this proposed cage system. The resulting crystal structure of **5** (Fig. 3) revealed that, as proposed, cage 5 contains three naphthyridine moieties connected by two trimethylbenzene units via six imine bonds. However, the solid state analysis also revealed features that differ from what might be expected based

on the idealized chemical structure provided in Fig. 1 or inferred from the solution phase ^{1}H NMR spectroscopic analysis. For examples, the three arms proved inequivalent in the solid state as inferred from their respective metric parameters, which stands in contrast to what is seen in solution. This apparent dichotomy could reflect the fact that in solution the three arms might are dynamic and thus become equivalent on the NMR time scale. Also noticeable is that the pyrrole-naphthyridine-pyrrole units, although near-planar, adopt a zig-zag conformation in the solid state. The naphthyridine nitrogen atoms point out from the macrobicyclic core while the pyrrolic NH hydrogen atoms point in the opposite direction. A single crystal X-ray diffraction analysis of cage **5** with solvents was carried out and revealed the location of solvent molecules (e.g., THF and water), which reside as guests both inside and outside of the cage. After removing the guests, the solvent accessible void volume is 2027.0 Å^3, which is ca. 32.6% of the total cell volume (6211 Å^3). A corresponding single crystal X-ray analysis of crystals of cage **5** studied in the absence of trapped solvents revealed that there are very small voids exists in crystallographic 'a'-axis. The corresponding space-filling model is provided in the ESI (Figure S18). Both presumed π···π (ca. 3.16 Å) and C-H···π (ca. 3.47 Å) interactions are accounted for in the solid state packing model as shown in the ESI (Figure S17). The resulting presumed loss in intramolecular hydrogen bonding interactions involving the pyrrole NH donor sites and naphthyridine accptors is probably compensated in terms of favorable entropy. In the event, as the result of these structural features the cryptand-like system **5** does not possess a large inner void in the solid state. Unfortunately, efforts to obtain diffraction grade crystals of cryptands **4** and **6** failed.

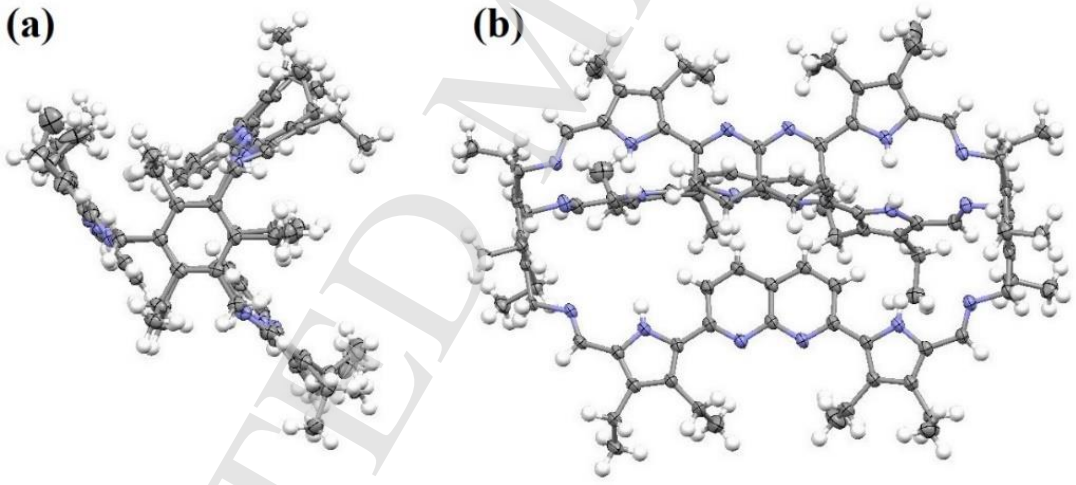

Fig. 3. Crystal structure of cryptand **5** viewed from top, (a) and side (b). The solvents molecules were removed for clarity.

Following seminal reports by Atwood and Cooper [13], increasing attention attention has been devoted to probing the gas adsorption features of porous amorphous cages [14]. However, little attention has been paid in this context to pyrrole-based macrocyclic systems. Recently, we demonstrated that the macrobicyclic imine-cages **2** and **3** could selectively adsorb CO_2 at 196 K [8]. Consistent with Mastalerz's earlier findings, the observed selectivity for CO_2 over other gases was ascribed to the presence of the polar functionalities within the core of the cage [15]. As detailed below, the present studies with cages **4**, **5** and **6**, respectively, are fully consistent with such a conclusion.

Typically, solid samples of cages **4**, **5** and **6** were subjected to gas sorption analysis using CO_2, N_2, H_2, O_2 and CH_4 as the probe gases; it was found that all three cages had the expected selectivity towards CO_2 [16]. As shown in Fig. 4, the calculated BET surface areas obtained using CO_2 were 160, 104 and 133 $m^2\ g^{-1}$ for cages **4**–**6**, respectively (see Supporting Information, Table S2). These values are considered to reflect the microporosity of each individual cryptand. In contrast, the H_2 uptake in each material was exceptionally poor, lending credence to the conclusion that the surface area of these cages is negligible. Apart from CO_2, a modest degree of adsorption was seen in the case of N_2 and O_2. Little (but detectable) methane adsorption was seen in spite of the fact that the critical diameter of CH_4 is smaller than CO_2 and should therefore be able to access the micropores (i.e., size exclusion should not apply). Thus, all cages appear to show a clear adsorption preference for the more polarizable CO_2 adsorbate. N_2, O_2 and CH_4 showed adsorption behaviour with moderate hysteresis, likely due to bottlenecks within the structures [17]. The sorption values achieved are comparable to those of many other [2+3] imine cryptands [13(c), 14], although BET surface areas as high as 918 $m^2\ g^{-1}$ have been noted previously in the literature [18]. To study the effect of desolvation on the structure of cages **4**, **5**, and **6**, PXRD studies were carried out with samples both as synthesized and after activation via solvent removal. The result data (cf. ESI Fig. S19) confirmed retention of bullk crystallinity upon desolvation and very small change in the metric symmetry in the case of cages **5** and **6**. Moreover, the simulated PXRD pattern for cage **5** generated using PLATON revealed a good, albeit not perfect, match between the simulated and experimental PXRD patterns. The small differences are ascribed to the crystalline quality of the bulk sample that is not considered as prisitine as that of the single crystals. On the other hand, the PXRD analysis revealed a lack of strong crystallinity in the case of cage **4**. Thus, in this latter case gas uptake could reflect contributions from both adsorption and absorption.

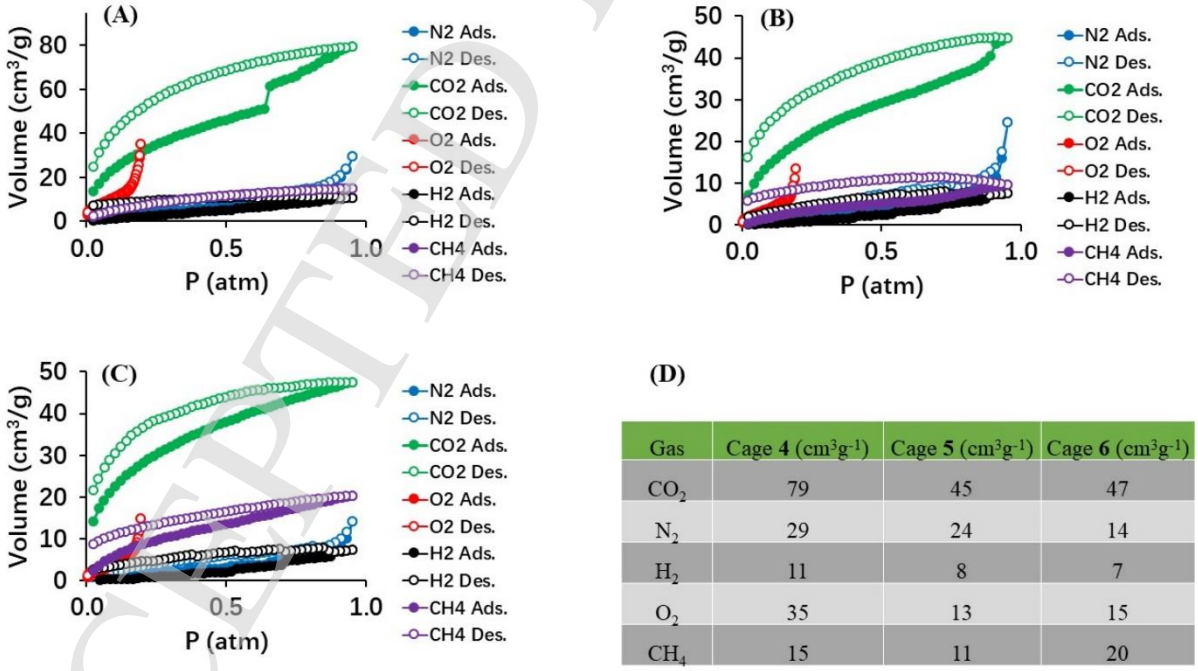

Gas	Cage **4** (cm^3g^{-1})	Cage **5** (cm^3g^{-1})	Cage **6** (cm^3g^{-1})
CO_2	79	45	47
N_2	29	24	14
H_2	11	8	7
O_2	35	13	15
CH_4	15	11	20

Fig. 4. Comparison of sorption isotherms for cage **4 (A)**, cage **5 (B)** ,and cage **6 (C)**, respectively. Closed circles represent adsorption and open circles show subsequent gas desorption. The N_2, H_2 and O_2 isotherms

were recorded at 77 K; those for CH_4 and CO_2 were recorded at 196 K. **(D)** Tabular listing of the maximum measured capacities.

In conclusion, we succeeded in synthesizing three cryptands (**4**, **5**, and **6**) in high yield through Schiff base condensation reactions between two dialdehydes (**7** and **8**) and two triamines (**13** and **14**). The resulting macrobicyclic cages were fully characterized by various spectroscopic methods, and in the case of compound **5**, by single crystal X-ray diffraction analysis. Gas adsorption studies in the solid state revealed the preference for CO_2 gas over other test gases (e.g., N_2, H_2, O_2, CH_4, respectively), a result ascribed to the presence of polar pyrrolic subunits within the central cores of these three molecular scaffolds. The present study thus serves to demonstrate how rational design of polypyrrolic macrobicyclic systems can yield systems with potentially interesting gas adsorption selectivities.

EXPERIMENTAL

General information

All chemicals used were purchased from Aldrich, TCI, Energy Chemicals, Adamas-beta® or Acros and used without further purification unless otherwise mentioned. All solvents used in the reactions were purchased from local suppliers and dried prior to use. Thin-layer chromatographic (TLC) analyses were carried out using silica gel pre-coated on glass sheets. Column chromatography was performed on silica gel of mesh size 200-300. ^{1}H NM and ^{13}C NMR spectra were recorded using a JEOL 400, Bruker 500, or 600 MHz instruments at room temperature and chemical shifts are reported in ppm using TMS or solvent residual signals as an internal reference standards. MALDI-TOF mass spectra were taken on a Bruker (Autoflex speed) matrix-assisted laser desorption ionization time-of-flight mass spectrometry. The data for single crystal X-ray diffraction analyses were collected on a Bruker/ARINAX MD2 diffractometer equipped with a MarCCD-300 detector at beam line station BL17B of Shanghai Synchrotron Radiation Facility (SSRF). Suitable single crystal was mounted on a Nylon loop with Paratone-N oil for diffraction at 100 K. All experiments were carried out using the radiation with a wavelength of 0.65295 Å (E = 19 keV), and the detector distance was 115 mm. For each dataset, 360 frames were collected by using ω-scans with an oscillation range of 1° and an exposure time of 1 s. Data collection was performed using the BlueIce software package. Cell refinements, data reductions and absorption corrections were carried out using the HKL3000 software package. All structures were solved by direct methods and refined by full-matrix least-squares on F2 using SHELXTL software. Non-hydrogen atoms were refined with anisotropic displacement parameters. Hydrogen atoms were calculated in ideal positions with isotropic displacement parameters set to 1.2 × Ueq or 1.5 × Ueq of the attached atoms. Contributions of highly disordered solvents were removed by SQUEEZE routine using PLATON. DISP instruction was used for all datasets. The crystal structure was rendered using the Mercury program downloaded from the Cambridge Crystallographic Data Centre (CCDC) [19]. CCDC-1937925 and CCDC-1952295 contain the supplementary crystallographic data for this paper. These data can be obtained free of charge from the Cambridge Crystallographic Data Centre [20].

General synthesis of 12

A mixture of **11** (36 mmol) [21] and $PdCl_2(PPh_3)_2$ (1.8 mmol) was purged under N_2 for 10 min before 150 mL dry dioxane was added. The resulting solution was treated with dry triethylamine (TEA; 90 mmol) at room temperature, followed by the dropwise addition of pinacolborane (54 mmol). The reaction mixture was then heated at 65 ℃ for 3 h before being cooled to room temperature. After removal of volatiles, the product was separated by column chromatography over silica gel eluting with PE/ ethyl acetate (EA), 30/1, v/v. This gave compound **12** in the form of reddish-brown oil which solidified at low temperature to yield a reddish-brown solid.

12: Yield: 50-70% as a reddish-brown solid. ^{1}H NMR (600 MHz, $CDCl_3$) δ 9.67 (s, 1H, -CHO), 9.25 (s, 1H, NH), 2.73 (q, *J* = 7.6 Hz, 2H, CH_2 alkyl pyrrole), 2.64 (q, *J* = 7.5 Hz, 2H, CH2 alkyl pyrrole), 1.31 (s, 12H, CH_3 alkyl boron ester), 1.23 (t, *J* = 7.6 Hz, 3H, CH_3 alkyl pyrrole), 1.14 (t, *J* = 7.5 Hz, 3H, CH_3 alkyl pyrrole). ^{13}C NMR (150 MHz, $CDCl_3$) δ 178.33 (s), 137.83 (s), 136.16 (s), 131.47 (s), 83.95 (s), 24.77 (s), 17.95 (s), 17.69 (s), 17.06 (s), 16.76 (s).

General synthesis of 8

To a 50 mL round-bottom flask was added 2, 7-dibromo-1, 8-naphthyridine (1 mmol), $Pd(OAc)_2$ (0.1 mmol), PPh_3 (0.2 mmol) and K_2CO_3 (3.3 mmol). Under an N_2 atmosphere, DMF (10 mL) and water (10 mL) were added through a syringe. Then, the mixture was heated to 85 ℃. After about 1 h, compound **12** (2.5 mmol) was dissolved in 10 mL DMF and added via a syringe pump over the course of 1 h. The reaction was stirred at the same temperature for another 23 h. The reaction mixture was allowed to cool to room temperature. The organic portion was extracted with DCM, washed with water 3 times, and the organic layer was then passed through anhydrous Na_2SO_4. After removal of the solvents and other volatiles, the crude reaction mixture was purified by silica gel column chromatography using PE/EA as the eluent, (30/1, v/v) to obtain compound **8** as a brown powder.

8: Yield: 45% as a brown powder. ^{1}H NMR (400 MHz, $CDCl_3$) δ 10.45 (s, 2H, NH), 9.82 (s, 2H, CHO), 8.18 (d, *J* = 8.5 Hz, 2H, naphthyridine), 7.81 (d, *J* = 8.5 Hz, 2H, naphthyridine), 2.85 (dq, *J* = 22.7, 7.6 Hz, 8H, CH_2 alkyl pyrrole), 1.29 (td, *J* = 7.6, 2.7 Hz, 12H, CH_3 alkyl pyrrole). ^{13}C NMR (100 MHz, $CDCl_3$) δ 178.48 (s), 155.46 (s), 153.17 (s), 137.71 (s), 137.55 (s), 132.82 (s), 129.41 (s), 127.87 (s), 120.78 (s), 119.45 (s), 18.08 (s), 17.64 (s), 17.01 (s), 15.80 (s). MALDI-TOF MS Calcd for $C_{26}H_{28}N_4O_2$ $[M]^+$ 428.536. Found: 428.531.

General synthesis of 4, 5 and 6

To a 500 mL round-bottom flask was charged compound **7** [7] (0.3 mmol). The flask was sealed with a septum and purged with N_2 for 20 min before adding 300 mL dry methanol. Under an N_2 atmosphere, (2,4,6-triethylbenzene-1,3,5-triyl)- trimethanamine (**13**) (0.2 mmol) in 50 mL methanol was added dropwise (roughly 5 seconds per drop) to the methanol solution of compound **7**. After completion of the addition, the mixture was stirred for another 48 h at room temperature. The resulting saffron yellow precipitate was filtered, and washed with methanol, followed by drying under vacuum to afford **4** as a saffron yellow powder. The synthetic

procedure for **5** and **6** was the same used to obtain **4** except that DCM was used to dissolve dialdehyde **8** instead of methanol before it was added to a methanol solution of **13** or **14**.

4: Yield: 84% as a yellow powder. ^{1}H NMR (600 MHz, $CDCl_3$) δ 11.51 (s, 6H, NH), 8.19 (s, 6H, imine), 7.60 (t, *J* = 7.9 Hz, 3H, pyridine), 7.31 (d, *J* = 7.9 Hz, 6H, pyridine), 4.79 (s, 12H, CH_2 benzene), 2.80 (d, *J* = 7.2 Hz, 12H, CH_2 benzene), 2.71 (dd, *J* = 15.0, 7.5 Hz, 12H, CH_2 alkyl pyrrole), 2.57 (dd, *J* = 15.1, 7.5 Hz, 12H, CH_2 alkyl pyrrole), 1.20 - 1.07 (m, 54H, CH_3 alkyl). ^{13}C NMR (150 MHz, $CDCl_3$) δ 150.59 (s), 149.61 (s), 144.31 (s), 136.91 (s), 133.32 (s), 132.10 (s), 130.76 (s), 125.87 (s), 124.55 (s), 116.43 (s), 57.59 (s), 23.83 (s), 18.11 (s), 17.70 (s), 16.88 (s), 16.53 (s), 15.33 (s). MALDI-TOF MS Calcd for $C_{99}H_{123}N_{15}$ $[M]^+$ 1523.178. Found: 1523.878.

5: Yield: 80% as a brown powder. ^{1}H NMR (600 MHz, $CDCl_3$) δ 10.18 (s, 6H, NH), 8.14 (s, 6H, imine), 7.91 (d, *J* = 8.4 Hz, 6H, naphthyridine), 7.56 (d, *J* = 8.4 Hz, 6H, naphthyridine), 5.11 (s, 12H, CH_2 benzene), 2.93 (d, *J* = 7.0 Hz, 12H, CH_2 alkyl benzene), 2.73 (dd, *J* = 14.6, 7.2 Hz, 12H, CH_2 alkyl pyrrole), 2.62 (d, *J* = 7.3 Hz, 12H, CH_2 alkyl pyrrole), 1.33 (t, *J* = 7.4 Hz, 18H, CH_2 alkyl benzene), 1.20 (t, *J* = 7.5 Hz, 18H, CH_3 alkyl pyrrole), 1.12 (t, *J* = 7.5 Hz, 18H, CH_3 alkyl pyrrole). ^{13}C NMR (150 MHz, $CDCl_3$) δ 155.88 (s), 153.29 (s), 149.48 (s), 143.46 (s), 136.57 (s), 132.95 (s), 129.86 (s), 128.66 (s), 128.36 (s), 127.27 (s), 118.10 (s), 58.18 (s), 23.45 (s), 18.25 (s), 17.04 (s), 16.94 (s), 16.35 (s), 15.72 (s), 14.14 (s). MALDI-TOF MS Calcd for $C_{108}H_{126}N_{18}$ $[M]^+$ 1676.322. Found: 1676.407.

6: Yield: 83% as a brown powder. ^{1}H NMR (600 MHz, $CDCl_3$) δ 10.53 (s, 6H, NH), 8.12 (s, 6H, imine), 7.90 (d, *J* = 8.5 Hz, 6H, naphthyridine), 7.49 (d, *J* = 8.5 Hz, 6H, naphthyridine), 3.76 (t, *J* = 7.0 Hz, 12H, CH_2 amine), 3.20 - 2.99 (m, 12H, CH_2 amine), 2.70 (dd, *J* = 15.0, 7.4 Hz, 12H, CH_2 alkyl pyrrole), 2.50 (dd, *J* = 15.0, 7.5 Hz, 12H, CH_2 alkyl pyrrole), 1.21 (t, *J* = 7.5 Hz, 18H, CH_3 alkyl pyrrole), 1.14 (t, *J* = 7.5 Hz, 18H, CH_3 alkyl pyrrole). ^{13}C NMR (150 MHz, $CDCl_3$) δ 155.45 (s), 152.87 (s), 149.57 (s), 136.15 (s), 130.22 (s), 129.12 (s), 127.99 (s), 126.41 (s), 119.16 (s), 117.87 (s), 62.63 (s), 57.38 (s), 18.30 (s), 17.55 (s), 16.72 (s), 15.76 (s). MALDI-TOF MS Calcd for $C_{90}H_{108}N_{20}$ $[M]^+$ 1469.994. Found: 1469.308.

Acknowledgements

Support for this work came from the Center for Supramolecular Chemistry and Catalysis of the Shanghai University. We thank the staff of Beamline BL17B at the National Facility for Protein Science Shanghai Synchrotron Radiation Facility for assistance during the single-crystal X-ray data collection.

Supporting information; CCDC

^{1}H NMR and ^{13}C NMR spectra, MALDI-TOF mass spectra and crystallographic data (Figs S1–S16) are given in the supplementary material. This material is available free of charge *via* the Internet. Crystallographic data have been deposited at the Cambridge Crystallographic Data Centre (CCDC) under CCDC numbers: 1937925 and 1952295.

REFERENCES

1. (a) MacDowell D and Nelson J. *Tetrahedron Let.* 1988; **29**: 385-386. (b) Skowronek P and Gawronski J. *Org. Lett.* 2008; **10**: 4755-4758. (c) Liu XJ, Liu Y, Li G and Warmuth R. *Angew. Chem. Int. Ed.* 2006; **118**: 915-918. (d) Mastalerz M. *Chem. Commun.* 2008; 4756-4758.
2. (a) Christinat N, Scopelliti R and Severin K. *Angew. Chem. Int. Ed.* 2008; **47**: 1848-1852. (b) Zhang G, Presly O, White F, Oppel IM and Mastalerz M. *Angew. Chem. Int. Ed.* 2014; **53**: 1516-1520. (c) Klotzbach S, Scherpf T and Beuerle F. *Chem. Commun.* 2014; **50**: 12454-12457.
3. Collins MS, Carnes ME, Nell BP, Zakharov LN and Johnson DW. *Nat. Commun.* 2016; **7**: 11052.
4. (a) Zhang G and Mastalerz M. *Chem. Soc. Rev.* 2014; **43**: 1934-1947. (b) Beuerle F and Gole B. *Angew. Chem. Int. Ed.* 2018; **57**: 4850-4878. (c) Mastalerz M. *Acc. Chem. Res.* 2018; **51**: 2411-2422.
5. Schick THG, Lauer JC, Rominger F and Mastalerz M. *Angew. Chem. Int. Ed.* 2019; **58**: 1768-1773.
6. Jin Y, Voss BA, Noble RD and Zhang W. *Angew. Chem. Int. Ed.* 2010; **122**: 6492-6495.
7. Setsune J-i and Watanabe K. *J. Am. Chem. Soc.* 2008; **130**: 2404-2405.
8. Wang F, Sikma E, Duan ZM, Sarma T, Lei CH, Zhang Z, Humphrey SM and Sessler JL. *Chem. Commun.* 2019; **55**: 6185-6188.
9. Setsune J-i, Toda M, Watanabe K, Panda PK and Yoshida T. *Tetrahedron Lett.* 2006; **47**: 7541-7544.
10. Trofimov BA. *Uspekhi Khimii*, 1989, **58**: 1703-1720.
11. (a) Shevchuk SV, Davis JM and Sessler JL. *Tetrahedron Lett.* 2001; **42**: 2447-2450. (b) Stark DG, Williamson P, Gayner ER, Musolino SF, Kerr RWF, Taylor JE, Slawin AMZ, O'Riordan TJC, Macgregor SA and Smith AD. *Org. Biomol. Chem.* 2016; **14**: 8957-8965. (c) Chen CY, Bocian DF and Lindsey JS. *J. Org. Chem.* 2014; **79**: 1001-1016.
12. (a) Davis RA, Carroll AR, Quinn RJ, Healy PC and White AR. *Acta Crystallogr. E.* 2007; **63**: o4076-o4076. (b) Zhang Z, Lim JM, Ishida M, Roznyatovskiy VV, Lynch VM, Gong HY, Yang X, Kim D and Sessler JL. *J. Am. Chem. Soc.* 2012; **134**: 4076-4079. (c) Anguera G, Kauffmann B, Borrell JI, Borrós S and Sánchez-García D. *Org. Lett.* 2015; **17**: 2194-2197. (d) Algi MP, Oztas Z, Tirkeş S, Cihaner A and Algi F. *J. Fluoresce.* 2017; **27**: 509-519.
13. (a) Tian J, Thallapally PK, Dalgarno SJ, McGrail PB and Atwood JL. *Angew. Chem. Int. Ed.* 2009; **48**: 5492-5495. (b) Kudo H, Hyashi R, Mitani K, Yokozawa T, Kasuga NC and Nishikubo T. *Angew. Chem. Int. Ed.* 2006; **45**: 7948-7952. (c) Tozawa T, Jones JTA, Swamy SI, Jiang S, Adams DJ, Shakespeare S, Clowes R, Bradshaw D, Hasell T, Chong SY, Tang C, Thompson S, Parker J, Trewin A, Bacsa J, Slawin AMZ, Steiner A and Cooper AI. *Nat. Mater.* 2009; **8**: 973.
14. Hasell T and Cooper AI. *Nat. Rev. Mater.* 2016; **1**: 16053.
15. (a) Schneider MW, Hauswald HJS, Stoll R and Mastalerz M. *Chem. Commun.* 2012; **48**: 9861-9863. (b) Schneider MW, Oppel IM and Mastalerz M. *Chem.-Eur. J.*, 2012, **18**: 4156-4160.
16. (a) Jin Y, Voss BA, Noble RD and Zhang W. *Angew. Chem. Int. Ed.* 2010; **49**: 6348-6351. (b) Jin Y, Voss BA, Jin A, Long H, Noble RD and Zhang W. *J. Am. Chem. Soc.* 2011; **133**: 6650-6658.
17. Nguyen PT, Fan C, Do DD and Nicholson D. *J. Phys. Chem. C*. 2013; **117**: 5475-5484.
18. (a) Beaudoin D, Rominger F and Mastalerz M. *Angew. Chem. Int. Ed.* 2017; **56**: 1244-1248. (b) Schneider MW, Oppel IM, Griffin A and Mastalerz M. *Angew. Chem., Int. Ed.* 2013; **52**: 3611-3615.
19. https://www.ccdc.cam.ac.uk/solutions/csd-system/ components/mercury/
20. https://www.ccdc.cam.ac.uk/structures/
21. Rana A, Lee S, Kim D, and Panda PK. *Chem.-Eur. J.* 2015; **21**: 12129-12135.

TOC

New cryptands were synthesised through Schiff base condensation reaction between dialdehydes and triamines. Gas adsorption studies in the solid state revealed a preference for CO_2 over other test gases (N_2, H_2, O_2, CH_4).